

# FIRST LEBT SIMULATIONS FOR THE BILBAO ACCELERATOR ION SOURCE TEST STAND

I. Bustinduy, D. de Cos, J. Feuchtwanger, J.L. Munoz, F.J. Bermejo, ESS-Bilbao, Spain  
 S. Lawrie, D. Faircloth, A. Letchford, J. Pozimski, STFC/RAL, Chilton, Didcot, Oxon, UK  
 S. Jolly, P. Savage, Imperial College of Science and Technology, UK  
 J.Back, Warwick University, UK  
 J. Lucas, Elytt Energy, Madrid, Spain  
 J.P. Carneiro, IkerBasque Foundation, Chicago, USA

## Abstract

The proposed multi-specimen Low Energy Transport System (LEBT) consists of a series of solenoids with tunable magnetic fields, used to match the characteristics of the beam to those imposed by the RFQ input specification. The design of the LEBT involves selecting the number of solenoids to use and their fixed positions, so that a set of fields that provides the desired matching can be found for any given conditions (different currents, input emittances, etc). In this work we present the first simulations carried out to design the Bilbao Accelerator LEBT, which were performed using several codes (TRACK, GPT, Trace2D). The best configuration is discussed and evaluated in terms of the degree of matching to the RFQ input requirements.

## INTRODUCTION

As a continuation of the ITUR ion source test stand [1], a front end test stand (FETS) for proton is being currently designed and constructed in Bilbao (Spain), comprising a Low Energy Beam Transport (LEBT), a Radio-Frequency Quadrupole (RFQ) [2] and a High Speed Chopper [3]. The aim is to produce chopped proton beams of up to 75 mA current, up to 2 ms pulse length, and 50 Hz repetition rate.

The aim of the LEBT, placed between the ion source and the RFQ, is to match the beam characteristics to the RFQ input specification. This paper summarizes the latest advances on the Bilbao Accelerator LEBT design. Several aspects of the current design status will be covered, including the magnetic structure, cooling system, and beam dynamics simulations.

## MAGNETIC STRUCTURE

The Bilbao Accelerator LEBT is composed of a series of solenoids placed at fixed positions, producing tunable magnetic fields. The number of solenoids used will be discussed later in this paper. Figure 1 shows the layout for the 4-solenoid configuration.

Following the work in [4], the solenoids present a smaller internal radius (involving more turns) at the ends than in the centre. This way, the magnetic field profile along the axis is flatter than the one achieved with a uniformly shaped solenoid, which would present a typical

### Beam Dynamics in High-Intensity Linacs

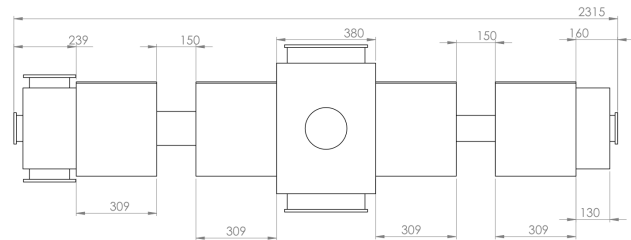


Figure 1: Proposed layout of the LEBT. The aperture of the first two magnets is 134 mm and 100 mm for the last two ones.

bell-shaped magnetic field profile. Besides, the variable radius approach creates a magnetic field that remains confined within the solenoid limits, avoiding perturbations on any nearby elements (e.g. other solenoids and the vacuum pump).

In order to save beam-line space, the proposed design includes the ability to nest dipoles and solenoids together. Therefore, the LEBT is composed of two types of elements:

- Two single solenoids, presenting an aperture of 134 mm, placed at the first and second positions of the LEBT.
- Two dipole-solenoid assemblies, composed by a solenoid integrated together with a set of two crossed (x-y) dipoles of the  $\cos\theta$  type (similar to typical structure used for superconducting magnets). The dipoles are capable of steering the beam to correct for misalignment of the beam line components, reaching a deflection of up to  $\pm 4^\circ$  for protons. These elements will be used at the third and fourth positions of the LEBT. The presence of the dipoles limits the aperture to 100 mm, which may be assumed due to the fact that the first two solenoids reduce the transverse dimensions of the beam.

The proposal for the solenoid design includes an iron yoke with ferromagnetic end plates. The preliminary analysis indicates that a relatively large current density is required in order to obtain the desired magnetic field. Therefore, we have opted for solenoids made of 16 independently cooled internal coils. Each of the coils will be cooled by an

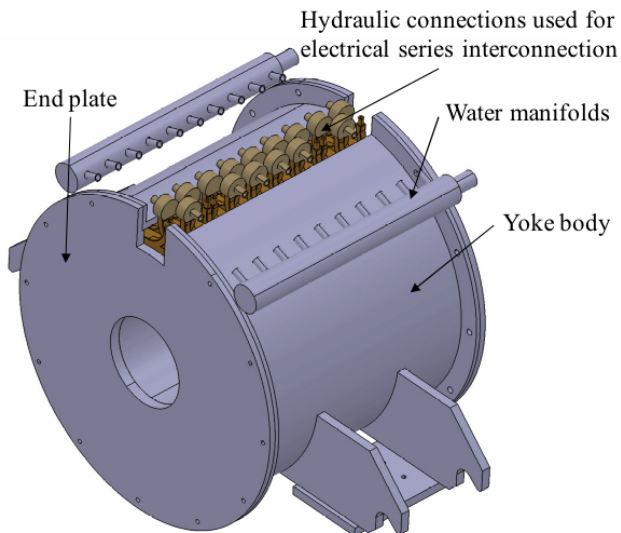


Figure 2: Isometric view of the solenoid assembly.

internal water flow in a hollow conductor, in parallel with the others. Electrically, the coils are connected in series, so that the same current flows through all of them. Figure 2 shows an isometric view of the solenoid.

In order to minimize the current of the power supply, we have opted for a small conductor, approximately 7 mm in length. An additional advantage of this solution is that the coil winding imperfections, like the layer jump, are smaller and the impact on the magnetic field quality is lower. The drawback of this choice is that a larger number of internal coils must be wound and series interconnected.

### Finite Element Model

The main objective of the magnetic design of the solenoids is to obtain a field profile along the axis that is as flat as possible. We have developed a Finite Element Model (FEM) of the solenoid to check its magnetic behavior. Both the models for a solenoid and a dipole-solenoid system have been implemented, the only difference between the models being that a larger aperture in the ferromagnetic front plate is required for the former. The model is axisymmetrical, and the coils are represented as current carrying areas. The on-axis longitudinal fields are represented in Fig. 3, for a circulating current of 300 A. The dipole-solenoid system (in blue) presents a field shape that decreases more abruptly near the edge. In addition, an increase of 3% of the magnetic induction is found at the center of the solenoid.

Finite element simulations show that the ferromagnetic material is not saturated at the highest operating currents, ensuring that the magnetic field generated will be linear with the drive current. In addition, the low carbon content ARMCO steel proposed for the solenoid casings has a very low coercivity, making the offset in the field due to the material's remanence low.

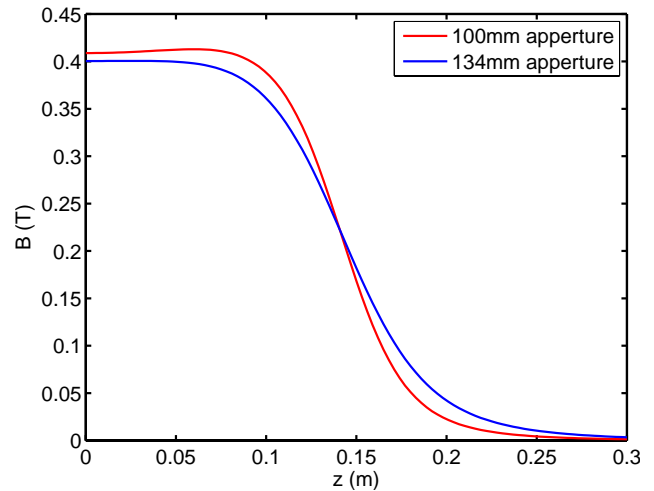


Figure 3: On axis field for the solenoid with and without steering dipoles, for a current of 300 A.

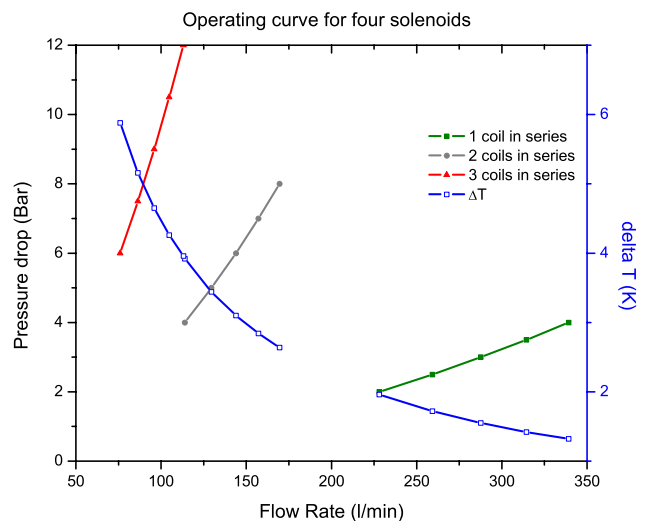


Figure 4: Operating curves for a four solenoid system. The solenoids are connected in parallel, and in each solenoid 1, 2 or 3 of the individual coils are connected in series. The blue trace corresponds to the temperature increase of the cooling water (y-axis) for the corresponding flow rate.

## COOLING SYSTEM

Each solenoid used in the LEBT presents a nominal rating of 30 V at 300 A (highest obtainable magnetic field under normal operating conditions). This translates into a maximum power of 9 kW per solenoid, and requires the flow of high current densities along the coils (up to 5 A/mm<sup>2</sup>), demanding the use of a hollow conductor refrigerated by an inner flow of water. The measurements performed by Elytt estimate the power dissipated per solenoid as approximately 8.1 kW. The discrepancy is attributed to the actual electrical resistivity of the coils being slightly less than the nominal value of 0.1  $\Omega$ .

The dissipated power calculated from the temperature increase of the cooling water and the flow rate is

### Beam Dynamics in High-Intensity Linacs

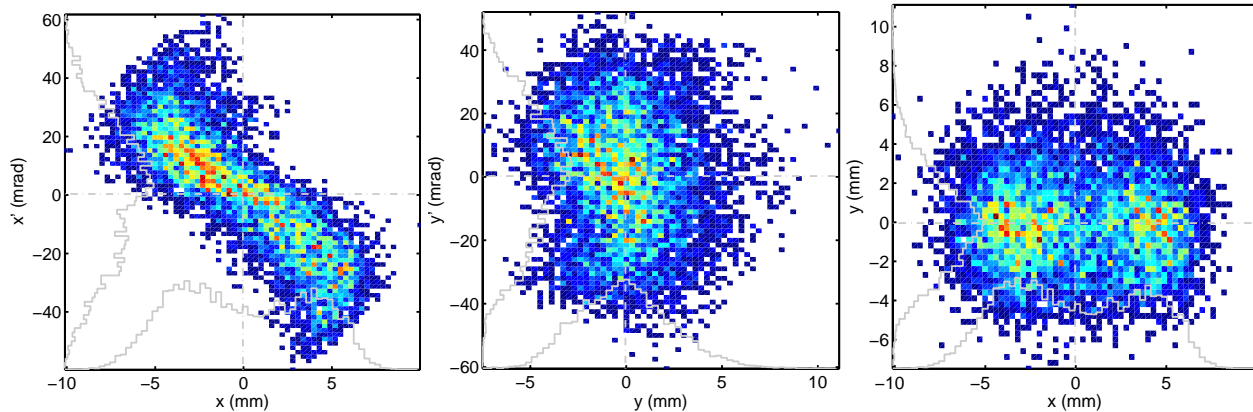


Figure 5: From left to right: Horizontal phase-space, vertical phase-space, and transverse distribution at the beginning of the LEBT. Pepperpot data measured  $\sim 400$  mm downstream of the cold box exit (the last exit plane of the ion source, after the 90 degree dipole), then tracked backwards to the entrance plane of the ISIS-FETS LEBT to provide the likely input beam at the start of the first LEBT drift and rescaled for 75 keV.  $T\alpha_x = 1.4366$ ,  $T\alpha_y = 0.0726$ ,  $T\beta_x = 0.2940$ ,  $T\beta_y = 0.1286$ . Normalized emittance is  $\sim 0.6 \pi$ -mm-mrad in both planes.

7.8 kW, assuming an average heat capacity for the water of  $4.184 \text{ J/gK}$ , and a mass density of  $1 \text{ g/cm}^3$ . This is in good agreement with the previous values, the small discrepancy being attributable to the power that is dissipated to the air. However, the water cooling system for a four solenoid LEBT has to be able to dissipate the nominal power of 36 kW for the total four solenoids.

### Operating Curve

From the experimental data presented by Elytt, we can study the hydraulics of the cooling system for different connection schemes. Figure 4 shows the operating curve—the pressure drop as a function of the flow rate—for a system comprised of four solenoids hydraulically connected in parallel, with each solenoid being internally arranged in sets of one, two, or three coils connected in series. Although the configuration with three coils in series is not feasible—16 (the number of coils in a solenoid) does not yield a whole number when divided by three—it is shown for illustrative purposes.

The curves in Fig. 4 show that by connecting one or two coils in series, the pressure drop of the system remains well below 10 bar. With three coils connected in series, the pressure drop can exceed 10 bar, while for four coils connected in series (not shown in the graph) the pressure drop would be higher than 10 bar at any flow rate. Pressure drops greater than 10 bar are considered too high and complicate the cooling system. Therefore, no more than 2 coils in the solenoids can be connected in series, any more would result in an excessively high pressure water feed requirement.

## VACUUM SYSTEM

Calculations to dimension the vacuum requirements for the LEBT are still underway. The system has to be able

to achieve a value of  $10^{-5}$  mbar at its inlet, which is the pressure required for the ion source to operate. At the same time, it has to be able to maintain a value of  $10^{-7}$  mbar, the maximum pressure acceptable for the RFQ to operate without arcing. This will be achieved by a set of 3 vacuum groups, one at each of the boxes in the system. The box at the inlet can house up to two 600 l/s turbopumps, and will have to take most of the gas load from the ion source. The central vessel can house one turbopump, of at most 2800 l/s and the last box can house up to two 600 l/s turbopumps, that are used to ensure that the pressure requirement for the RFQ is met.

## BEAM DYNAMICS SIMULATIONS

In order to find the best LEBT configuration, various preliminary studies were carried out to determine certain aspects of the design, such as finding the critical distances that cannot be surpassed in the final layout, and establishing the number of solenoids that conform the system. The simulations, performed using GPT [5], TRACK [6] and Trace2D [7] computer codes, took into account diverse scenarios, such as varying from 2 to 4 the number of solenoids; using different input particles ( $\text{H}^+$ ,  $\text{H}^-$ ,  $\text{D}^+$ ); and different beam currents (from 0 mA up to 100 mA, with no charge neutralization). In all cases, the solenoid positions were fixed, since the projected LEBT it is not expected to contain any movable parts in its final configuration.

Setting the defining parameters of a LEBT system consists basically of matching the transverse characteristics of the beam (defined in terms of the Courant-Snyder parameters as  $[T\alpha_x, T\beta_x, T\alpha_y, T\beta_y]$ ) to the RFQ input specification, which maximizes the transmission of the beam and minimizes its emittance growth. Strictly speaking, four system variables (magnetic field values, solenoid positions) are required to adjust the beam. In certain cases, if the beam

Table 1: Measured parameters at the RFQ input for different ion currents. Only a representative fraction of the simulations is presented here. Note that I(mA) refers to the non-neutralized current.

I (mA)	Software	B1 (T)	B2 (T)	B3 (T)	B4 (T)	$T\alpha_x$	$T\alpha_y$	$T\beta_x$ (m/rad)	$T\beta_y$ (m/rad)	$\Delta n\epsilon_x$ (%)	$\Delta n\epsilon_y$ (%)	RFQ Transmission (%)
0	GPT	0.184	0.165	0.087	0.317	0.564	0.755	0.0377	0.0391	34.84	27.95	79.8
	TRACK	0.256	0.106	0.060	0.328	0.650	0.660	0.0309	0.0302	38.98	34.71	84.0
2	GPT	0.365	0.050	0.018	0.035	0.732	0.672	0.0336	0.0331	30.59	16.94	89.2
	TRACK	0.272	0.094	0.077	0.329	0.740	0.630	0.0312	0.0297	47.35	41.28	81.1
4	GPT	0.353	0.0719	0.008	0.350	0.829	0.7661	0.0333	0.0323	34.43	26.34	87.1
	TRACK	0.282	0.101	0.079	0.331	0.810	0.610	0.0319	0.0299	54.05	42.93	80.0
6	GPT	0.350	0.100	0.025	0.350	0.956	0.789	0.0339	0.0364	39.22	29.34	85.9
	TRACK	0.292	0.086	0.108	0.327	0.750	0.520	0.0303	0.0285	65.77	47.86	76.9
8	GPT	0.331	0.131	0.008	0.350	0.878	0.728	0.0326	0.0327	51.33	39.82	82.9
	TRACK	0.300	0.117	0.076	0.336	0.660	0.690	0.0303	0.0292	44.01	77.43	73.8
10	GPT	0.333	0.145	0.042	0.350	0.911	0.685	0.0329	0.0346	58.74	36.00	81.3
	TRACK	0.302	0.141	0.049	0.341	0.750	0.660	0.0309	0.0293	55.73	70.86	73.1
20	GPT	0.339	0.195	0.089	0.353	0.822	0.523	0.0346	0.0353	79.55	35.71	72.5
	TRACK	0.351	0.189	0.050	0.354	0.850	0.600	0.0309	0.0334	60.75	49.50	75.8
30	GPT	0.340	0.234	0.098	0.362	0.769	0.397	0.0354	0.0404	72.97	36.98	67.0
	TRACK	0.378	0.215	0.140	0.354	0.510	0.350	0.0295	0.0325	54.05	52.78	68.9
40	GPT	0.308	0.275	0	0.384	0.613	0.243	0.0355	0.0602	68.65	46.80	54.3
	TRACK	0.392	0.250	0.180	0.361	0.180	0.190	0.0453	0.0308	55.73	54.43	54.3
50	GPT	0.295	0.281	0	0.390	0.425	0.125	0.0327	0.0687	83.21	58.95	43.5
	TRACK	0.392	0.266	0.180	0.370	0.010	0.040	0.0416	0.0300	75.82	69.21	46.1
60	GPT	0.375	0.244	0.195	0.355	0.394	0.298	0.0361	0.0568	68.32	52.35	43.2
	TRACK	0.400	0.280	0.200	0.370	0.130	0.280	0.0490	0.0430	95.91	84.00	40.2
70	GPT	0.400	0.269	0.212	0.369	0.076	0.251	0.0417	0.0648	95.70	97.63	35.1
	TRACK	0.400	0.290	0.220	0.375	0.000	0.220	0.0548	0.0570	105.96	93.86	31.8

is very axisymmetric and stable, one can do this with just two solenoids. However, the Bilbao Accelerator LEPT is expected to work with different particle species, and therefore the initial beam conditions are diverse and hard to predict. On the other hand, the beam created by the  $H^-$  Penning source is not expected to be cylinder symmetric, i.e. the emittances will be different in both planes and the beam becomes highly divergent very quickly.

So as a result, the 2 solenoid configuration was considered as very unsafe, as it only allows to achieve a good focusing for very certain beam characteristics. On the other hand, 3 solenoids provide a good matching in most of the cases, as long as only one certain specimen is used, but 4 solenoids are considered to be necessary in order to achieve the desired beam characteristics in every case.

#### 4D Magnetic Field Calculations

In order to confirm the validity of the proposed layout, we have designed an algorithm that finds the four magnetic fields that match a real  $H^-$  input beam distribution, measured by the ISIS-FETS project pepperpot [8] (see Fig. 5 for details). The beam dynamics simulations involved in the search were performed with GPT.

Contrary to the brute-force method of exploring the whole set of possible combinations, which is extremely time consuming, the proposed methodology consists on exploring the 4D universe of solenoid fields by following a path that minimizes the relative distance between

the Courant-Snyder parameters obtained at the entrance of the RFQ and the ones specified by the RFQ design: [ $T\alpha_{xo} = 1.008$ ,  $T\alpha_{yo} = 0.978$ ,  $T\beta_{xo} = 0.027$  m/rad,  $T\beta_{yo} = 0.0305$  m/rad]. The distance is defined as follows:

$$d = \sqrt{\left(\frac{T\alpha_x}{T\alpha_{xo}} - 1\right)^2 + \left(\frac{T\beta_x}{T\beta_{xo}} - 1\right)^2 + \dots} \quad (1)$$

where  $T\alpha_x$  represents the calculated parameter, and  $T\alpha_{xo}$  stands for the same parameter desired at the entrance of the RFQ. The distance takes into account the relative differences between the four parameters, ensuring that  $T\alpha$  and  $T\beta$  contributions weight the same despite presenting values two orders of magnitude apart.

For a given  $[B_1, B_2, B_3, B_4]$  configuration, the proposed algorithm explores all combinations of each solenoid magnetic field ( $B_i - \delta B$ ,  $B_i$ ,  $B_i + \delta B$ ) in its vicinity, i.e. a total of  $3^4 = 81$  possibilities. In case a shorter distance is found in any of the obtained 81 leaves, we move to it and start the next iteration. If no better solution is found after any iteration, the algorithm will stay in the same leaf, but  $\delta B$  will be refined, in order to explore nearer solutions. The script will continue until the distance is below a given threshold, or  $\delta B$  gets below a realistic achievable value. The actual implementation has been divided in two steps: first, a good seed is found by means of a brute-force algorithm using a coarse  $\delta B$ ; second, once an appropriate set of  $B$  parameters is found, the refining algorithm is launched. Only solutions in which 100% of the particles are successfully transported

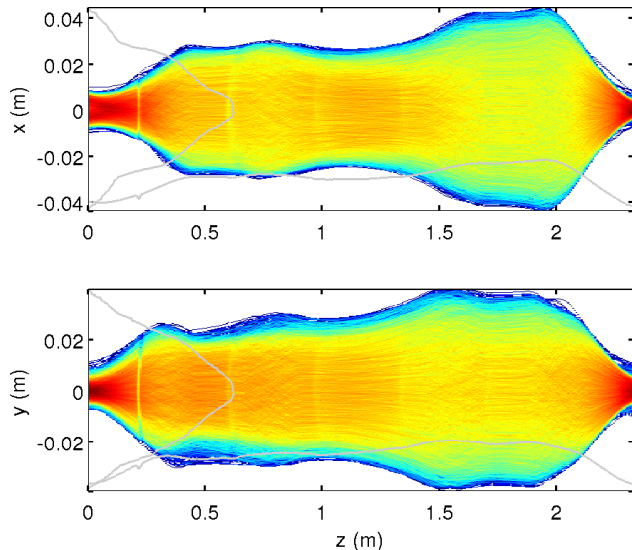


Figure 6: Horizontal and vertical projection of Beam Trajectories going through the LEBT, for a 70 mA beam current.

along the LEBT are considered.

The main drawback in the presented algorithm comes from the fact that it will not discern between strong and weak focusing solutions. Although the differences are clear between these two main categories by means of visual inspection, a general purpose implementation is far from being straightforward.

## RESULTS

The algorithm proposed above was launched to find the optimal magnetic fields for different input beam currents of  $H^-$ . The results are summarized in Table 1. The set of solenoid fields, the resulting Courant-Snyder parameters at the entrance of the RFQ, and the emittance growth at the LEBT output are presented for each current. An extra column is included presenting the transmission at the end of the RFQ using the calculated parameters as an input, which was simulated with Alan Letchford's RFQSIM. Simulations with GPT and TRACK were performed using the input distribution presented in Fig. 5 with 10k macroparticles. GPT results were obtained using the algorithm described above while TRACK matching was performed using preliminary matching results from Trace2D with an additional finer manual matching.

The results show quite good agreements between the optimal RFQ input parameters ( $T\alpha_{x0} = 1.008$ ,  $T\alpha_{y0} = 0.978$ ,  $T\beta_{x0} = 0.027$  m/rad,  $T\beta_{y0} = 0.0305$  m/rad) and the ones achieved for each current, up to about 10 mA. At higher currents, both the emittance growth along the LEBT and the particle loss in the RFQ begin to take off. The trajectories of the 70 mA current extreme case are represented in Fig. 6 where density of trajectories is represented by a logarithmic cold-hot color-scale, where warmer colors denote higher density of trajectories than the cooler ones.

### Beam Dynamics in High-Intensity Linacs

However, it must be noted that all the simulations were performed without taking into account any charge neutralization in the LEBT, which would decrease the beam current by a large factor. For example, a 90% neutralization applied to the maximum expected current of 75 mA will result in an actual current of 7.5 mA along the LEBT, which presents much better results (see the 8 mA row).

## CONCLUSIONS AND FUTURE WORK

We have presented the current status of the Bilbao Accelerator multi-specimen LEBT layout, including the magnetic structure, cooling and vacuum systems. An algorithm to find the values of the solenoid magnetic fields for different currents has been proposed, which can easily be extended to other optimization problems. The results are acceptable for low currents, which represent realistic scenarios once charge neutralization is taken into account.

As future work, the simulations will also be extended to other species, and refined once we obtain experimental data from the ITUR [1] project. Other lines of research, such as comparing the results with those obtained with TRACK [6] and more refined methods [9], are contemplated.

## REFERENCES

- [1] I. Bustinduy, et al., "First Simulation Tests For The Bilbao Accelerator Ion Source Test Stand" Proceedings of IPAC10, Kyoto, Japan, THPEC068, (2010).
- [2] D. de Cos, et al., "Beam Dynamic Studies On The Radio-Frequency Quadrupole For The Bilbao Accelerator" Proceedings of IPAC10, Kyoto, Japan, THPEC069, (2010).
- [3] I. Bustinduy et al, "Multiparticle Beam Dynamics Simulations for the ESS-Bilbao Superconducting Proton Accelerator", SFR2009, Berlin, Germany, THPPO099, pp. 869–870, (2009).
- [4] J. Pozimski, A. Letchford, J. Back, Dan Faircloth, S. Jolly, "Particle Dynamics Calculations and Emittance Measurements at the FETS", Proceedings of LINAC 2006, Knoxville, Tennessee USA, TUP066 (2006).
- [5] M.J. de Loos, S.B. van der Geer, Nucl. Instr. and Meth. in Phys. Res. B, Vol. 139, (1997) pp. 481.
- [6] V.N. Aseev, P.N. Ostroumov, E.S. Lessner and B. Mustapha, "Track: The New Beam Dynamics Code," Particle Accelerator Conference, 2005. Proceedings of PAC 2005, vol., no., pp. 2053- 2055, 16-20 May 2005.
- [7] Trace2D, Los Alamos Accelerator Code Group (LANL), <http://laacg1.lanl.gov/laacg/services.phtml>.
- [8] A. Letchford, et al., "Status Of the RAL Front End Test Stand", Proceedings of IPAC10, Kyoto, Japan, MOPEC075, (2011).
- [9] N. Chauvin, et al., "Final Design Of The IFMIF-EVEDA Low Energy Beam Transport Line", Proceedings of PAC09, Vancouver, BC, Canada, TH5PFP004, (2009).